Heliyon 5 (2019) e02824

Contents lists available at ScienceDirect

Heliyon

journal homepage: www.heliyon.com

Research article

In-vivo performance of plasma-sprayed CaO–MgO–SiO_2-based bioactive glass-ceramic coating on Ti–6Al–4V alloy for bone regeneration

Mengjiao Zhang [1], Ximing Pu [1], Xianchun Chen [*], Guangfu Yin

College of Materials Science and Engineering, Sichuan University, Chengdu, 610064, PR China

ARTICLE INFO

Keywords:
Materials chemistry
CaO–MgO–SiO_2 glass-ceramic coating
Ti–6Al–4V alloy
Osseointegration
Osteoinductivity
Osteogenesis

ABSTRACT

The CaO–MgO–SiO_2-based bioactive glass-ceramic coating (named M2) on Ti–6Al–4V alloy has been proven to behave well *in vitro*. But how to make full sense of its performances in terms of osteogenesis and osseointegration *in vivo* matters very much. For this, the M2-coated Ti–6Al–4V cylinders were prepared by atmospheric plasma spraying (APS) and implanted into New Zealand rabbit for 1, 2 and 3 months, respectively, by setting commercial HA-coated Ti–6Al–4V as the control. It is encouraging that, the two groups bonded with the surrounding tissues stably and newly formed bone grew towards or around the implants after 3-month implantation according to radiographic images. From the histological sections, it is obvious that, compared to the control, the M2-coated implant was more favorable for the osteogenesis and neo-*vascularisation* in the whole experimental process and demonstrated a better osseointegration with the host bone, indicating the former possessed better osteoconductivity, osteoinductivity and osteogenic ability. The study indicated that the M2-coated Ti–6Al–4V implant exerted a great potential to substitute the commercial HA-coated Ti–6Al–4V implant in repairing load-bearing bone defects.

1. Introduction

Bioceramics, especially calcium phosphate ceramics, due to their good biocompatibility and osteoconductivity, have been widely used for bone tissue repair in orthopedic and dental applications [1]. Representative of these ceramics is hydroxyapatite (HA, $Ca_{10}(PO_4)_6(OH)_2$), which is chemically and structurally equivalent to the mineral phase of natural bones and is thereby considered as an excellent bone substitute material. However, the inherent shortcomings of HA are its low fracture toughness and high Young's modulus, which limit its applications to implant coatings or situations of low mechanical load application, unless combined with other materials offering better mechanical properties. Thus, to improve the rate of implant fixation and prolong its longevity, nearly all bone and tooth implants are presently made from metal alloys coated with HA [2, 3, 4, 5], and one of the most accepted and commercial bioactive coatings is the plasma-sprayed HA coating on Ti–6Al–4V alloy [6]. Yet, the HA coating suffers from poor adhesion to the Ti–6Al–4V substrate because of the significant difference in their coefficient of thermal expansion (CTE). Besides, the clinical performance of HA coatings is plagued by certain adverse reactions found *in vitro* and *in vivo*, low crystallinity and coating's poor mechanical properties, which result in degradation, peeling, and eventual implant failure in long-term *in vivo* conditions [6, 7, 8]. Therefore, to find a new replacement for HA coating is a meaningful thing.

New bone formation was markedly dependent on the chemical composition of the bioactive ceramic [9]. Mg-containing silicate ceramics were found to meet the requirement of bone regeneration more than calcium phosphate (Ca–P) bioceramics. Ionic dissolution products from Ca-, Mg-, Si-containing bioceramics possessed the ability of regulating the growth and metabolism of bone-related cells. In essence, Ca, Mg and Si ions could activate the expression of bone related genes such as bone morphogenetic protein (BMP) and vascular endothelial growth factor (VEGF) to stimulate bone formation and angiogenesis [10, 11, 12, 13, 14, 15, 16, 17, 18, 19, 20, 21]. In our previous researches [22, 23], a novel CaO–MgO–SiO_2-based bioactive ceramic M2 (43.19% CaO-7.68% MgO-49.13% SiO_2 (wt%)) was firstly synthesized and deposited onto Ti–6Al–4V alloy using atmospheric plasma spraying (APS) system. Compared with commercial HA coating, a more than twofold increase in the bonding strength of M2 coating to Ti–6Al–4V substrate was obtained owing to its CTE closer to Ti–6Al–4V alloy. The study in vitro showed that

* Corresponding author.
E-mail addresses: kfwcxc@163.com, chenxianchun@scu.edu.cn (X. Chen).
[1] First and second author contributed equally.

https://doi.org/10.1016/j.heliyon.2019.e02824
Received 4 July 2019; Received in revised form 17 October 2019; Accepted 4 November 2019

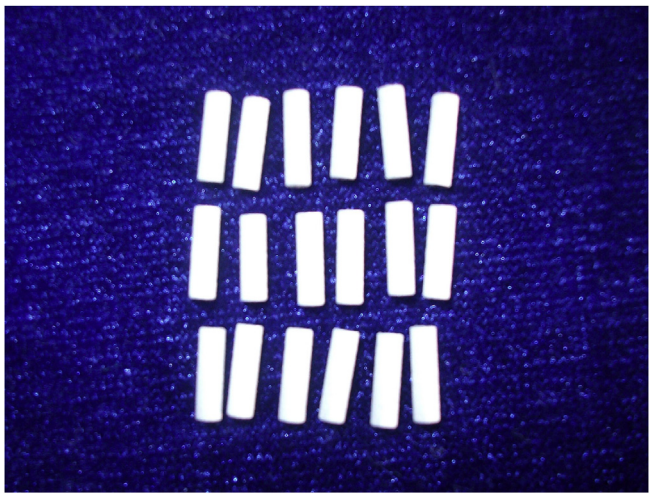

Fig. 1. The coatings/Ti–6Al–4V substrate composition cylindrical samples used in experiments *in vivo*.

M2 coating could induce bone-like carbonated apatite formation in SBF, which was an essential condition for Si-based biomaterials to bond to living bone directly after implantation into a host body [13, 14]. Furthermore, it could stimulate the proliferation and differentiation of osteoblasts, displaying good bioactivity and cytocompatibility *in vitro*.

Once the material has passed through the above tests *in vitro*, the next step prior to clinical trials is its evaluation in animals, since the complexity of physiological system *in vivo* can never be simulated by any culture assay *in vitro*. Thus, in this study, a rabbit femoral bone defect model [10, 24] was used to evaluate the tissue responses to M2 coated Ti–6Al–4V cylinders by radiography and histological examination, with commercial HA coated Ti–6Al–4V alloy as a control. Besides, the probable mechanism of bone tissue deposition and bone bonding to the novel implant was also explored.

2. Materials and methods

2.1. Materials

M2 powders and coating on Ti–6Al–4V substrate were prepared as described previously [23]. In brief, M2 powders were synthesized by the sol-gel method firstly, and then they were deposited onto Ti–6Al–4V substrate to obtain cylindrical pieces by APS system. The as-sprayed M2 coatings were ultimately heat-treated at 800 °C for 6 h in atmospheric environment.

According to Chinese national standard GB/T16886 [25], M2 coated Ti–6Al–4V cylinders with diameter of 2.0 mm and length of 6.0 mm (Φ 2 mm × 6 mm) (Fig. 1) were used as implants in a rabbit femoral defect model. The commercial HA coated Ti–6Al–4V cylinders with the same size were supplied by the National Engineering Research Center for Biomaterials of China, and served as control material.

Before implantation, the pieces of cylindrical implants were sterilized by autoclaving for 30 min at 121 °C.

2.2. Experimental animals and operative procedure

Animal experiments were conducted following the standards established by the Animal Research Committee of the State Key Laboratory of Oral Diseases and West China School of Stomatology, Sichuan University (approval number: SKLODLL2013A118). Briefly, 48 healthy New Zealand white rabbits weighing about 3.0 kg each were used to evaluate bone-regeneration ability in vivo of M2 coated Ti–6Al–4V cylinders in rabbit femur. They were randomly distributed into six groups of 8 animals each: (i) three groups for intraosseous implantation of M2 coated Ti–6Al–4V cylinders and the other (ii) for the control implantation of 1, 2 and 3 months (control group), respectively.

All the rabbits were purchased from the Laboratory Animal Center of West China Medical School, Sichuan University, and maintained in quarantine for two weeks before surgery. They were placed in individual cages under controlled conditions (room temperature 20 ± 0.5 °C, relative humidity 55 ± 5% and illumination with a 12 h/12 h of light/darkness photoperiod). All the animals had free access to a full rabbit's special fodder and libitum added water, without restriction of movement, *according to Chinese national standard GB/T16886* [25].

Surgery was performed under rigorously aseptic conditions and general anaesthesia induced by intramuscular injection of 20 mg/kg sodium pentobarbital provided by West China Hospital, Sichuan University). The femur was sterilized and exposed through a medical incision. Two bone holes of approximately 2.2 mm in diameter were drilled through the cortical bone using a surgical electronic drill (Fig. 2a) under a fixed speed of 600 rpm and profuse irrigation with sterile saline solution to cool. Before the insertion of the implants, the hole was irrigated with saline to remove the shards of bone. To make the implants contact with bone marrow, they were pressed as tightly as possible using finger pressure, followed by closing the muscle fascia and skin with nylon sutures. Subsequently, the wounds were moistened with iodine solution, as shown in Fig. 2b, and all animals received intramuscular injection of penicillin 10,000 units immediately. The animals were allowed to recover from anesthesia in the operation room under a heating lamp before being housed individually in the cages. Post-operatively, wounds were inspected daily for clinical signs of complications or adverse reactions and to monitor healing.

2.3. Double fluorescence labeling

Double fluorescence labeling was carried out for evaluation of osteogenesis and bone remodeling during the healing procedure. This technique allows marking the period of bone remodeling in agreement with the different colors of the markers [10]. For 3-month implantation,

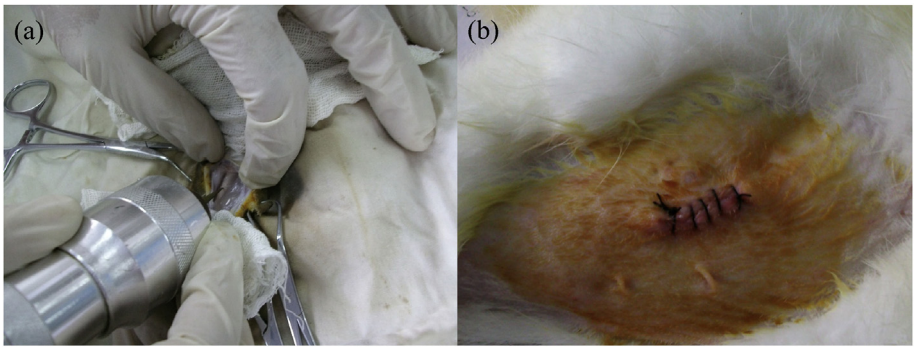

Fig. 2. Photographs about surgical process. (a) Drilling bone hole defect with a surgical electronic drill; (b) Sutured wound.

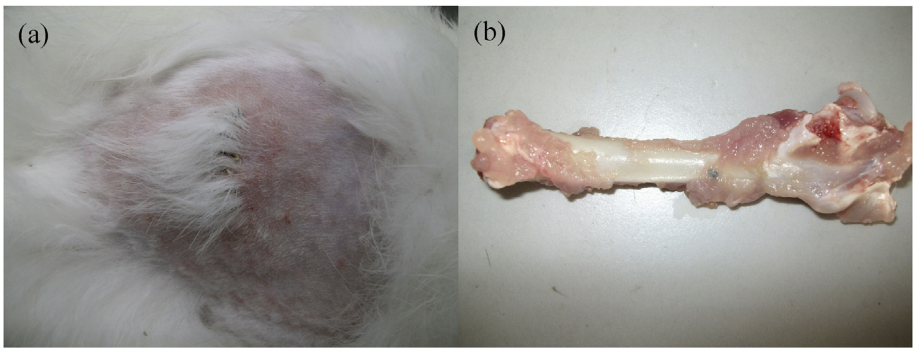

Fig. 3. Macroscopic appearance of (a) the wound healed, and (b) implants together with surrounding tissue, at 1 month after implantation.

tetracycline (20 mg/kg, Sigma) used as the first label was performed at 13 and 14 days before sacrificing the rabbits by an subcutaneous injection, and calcein (10 mg/kg, Sigma) as the second label was injected 3 and 4 days before sacrificing. These doses were dissolved in 0.9% sterile saline solution.

2.4. Radiological and histological evaluation

At predetermined time, all the animals were pharmacologically euthanized under general anaesthesia by an overdose of sodium pentobarbital, with the femoral condyles and diaphyses removed.

After sacrifice, standardized radiographs (Philips Easyvision 4.2, Philips Medical Systems, Brussels, Belgium) of femurs were taken to identify the stability and positions of the implants in bone femurs for morphological study.

To prepare hard-tissue slices for histological investigations, the samples, with soft tissue cleaned, were fixed in neutral buffered formaldehyde solution of 10 vol% (pH value = 7.2) for 30 days firstly, and then rinsed in tap water for 12 h. The fixed samples were dehydrated in graded series of alcohols from 70% to 100%, cleared with xylene, and subsequently embedded in polymethylmethacrylate resin. After hardening, the obtained samples were cut into 100-μm-thick sections perpendicular and parallel to the longitudinal axes of the implants under cooling water with a sawing microtome (Germany, Leica SP1600). The longitudinal and lateral sections were then glued onto a plastic support and polished to 50 μm in thickness and were finally stained with toluidine blue staining. All the bone histological sections were analyzed under light and fluorescent microscope (CX21, Olympus, Tokyo, Japan).

2.5. Statistical analysis

The results are presented as Means ± SD (n = 6). Analysis of the results was carried out by using one-way analysis of variance (ANOVA) and Bonferroni's post-test. A p value <0.05 was considered statistically significant.

3. Results and discussion

3.1. Clinical observations

For bone implant materials, it is critical to investigate their performance *in vivo* in host bone using a standardized animal model [10, 26]. In this study, a New Zealand white rabbit femoral bone defect model was employed to evaluate the osteogenesis ability and osseointegration *in vivo* of M2 coated Ti–6Al–4V alloy implants. The observations of commercial HA coated Ti–6Al–4V alloy employed as the control material could confirm its status as a biocompatible and osteoconductive implant and provide evidence for suitability of the rabbit femur model to evaluate osteoconductivity and osteointegration.

After operation, all the rabbits recovered quickly from the surgical procedures. No signs of noticeable surgical site infections, or adverse tissue reactions were observed around the implanted cylinders throughout the experiment. A typical example lay in the case of macroscopic evaluation of 1-month samples implanted in the bone cavities of rabbit femurs, as shown in Fig. 3, no obvious complications were noted in the animals. The wounds had healed well without dehiscence, skin ulceration and implant exposure around cylinders or osteosynthesis (Fig. 3a). Post-mortem macroscopic study did not show macroscopic tissue necrosis, effusion, or suppurative tissue infection in the peri-implant soft tissue. Neither displacement of implants nor necrosis of surrounding bone tissue was found. In addition, the cylinder implants were covered with normal healthy muscle tissue (Fig. 3b), indicating no visible harm to the soft tissue.

No implants instability and gap between implants and bone defects were observed through radiographic study after implantation for 1 month (Fig. 4), showing an intimate and clear material-bone interface in both groups. Moreover, the radiographs also confirmed that both types of implants had been successfully placed in the burr holes, penetrating the cortex into the bone marrow of the femur.

Host inflammatory response to implantation procedure and implant is an important and common type of foreign body reactions. In the initial

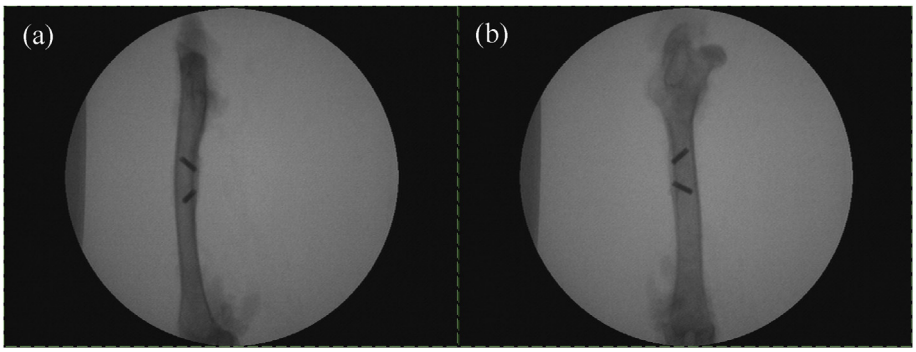

Fig. 4. X-RAY diagram of implants. (a) Positive; (b) Side.

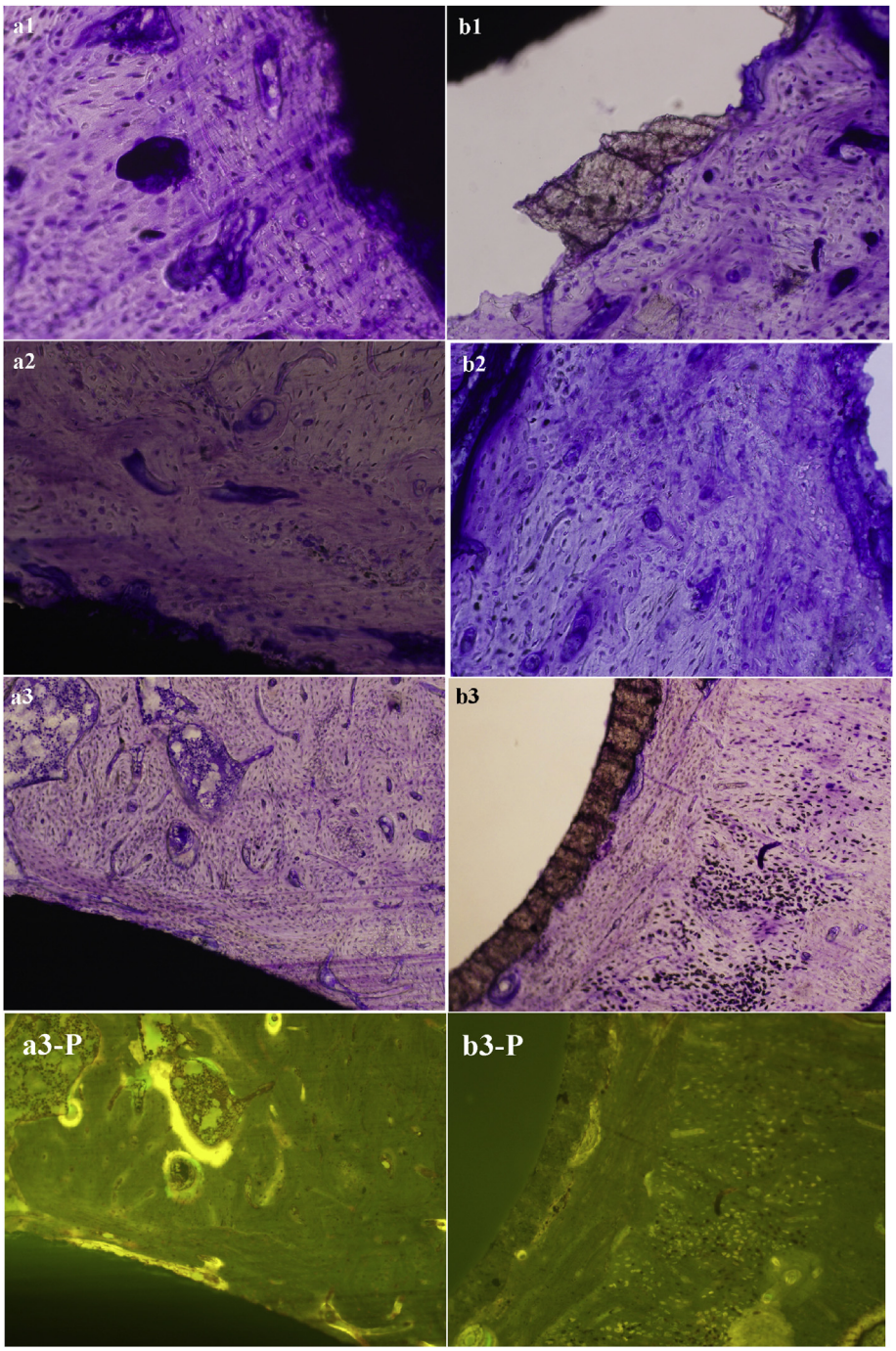

Fig. 5. Optical microscopy photograph of hard tissue biopsy of M2 and HA coating after toluidine-blue surface staining (×200). a1-a3 show the results of experimental group implanted for 1, 2 and 3 months, and b1-b3 are for HA coating group harvested at 1, 2 and 3 months, resepectively. Fig. a3-PL and b3-PL are labeled by tetracycline and calcein at 3 months.

period of implantation, inflammatory reaction and vascular congestion would appear in the local position, gradually decreased and disappeared completely with time. This phenomenon was attributed to normal body's rejection of the implanted tissue, which was also called the normal inflammatory response [27, 28]. This transient inflammatory response to implant and surgical trauma could be completely resolved within a short term, about 42 days as reported in the literature [29]. Williams [30] also declared that any biomaterials implanted in the body would cause inflammatory reaction of some degree. And its degree and duration directly affected the subsequent implantation stability and final effectiveness of the implanted prosthesis [31, 32]. On the other hand, numerous documents revealed that the outstanding biocompatibility and bioactivity of the tested materials were critical to reduce inflammatory response and facilitate osteogenesis and osteointegration process [32, 33]. In this research, the inflammatory response to M2 coated Ti–6Al–4V alloy implants was not observed at 1 month time point, which might be the major reason why the animals recovered rapidly from the surgery in this study.

Tissue-biomaterial process was a surface phenomena governed by surface properties. From a clinical point of view, ideal bone substitute biomaterial should possess excellent bioactivity and biocompatibility for osteogenesis and osteointegration [15, 30, 34]. Surface modification

could add biologically active and compatible functionality onto the bio-inert Ti-based implant surfaces, which improved its osteogenesis and bioactive bone-bonding ability and finally gave rise to favorable bone regeneration and osseointegration. By now, various surface modification methods were developed [2, 35, 36, 37]. Of these, depositing a coating with wonderful biological characteristics on Ti-based implant surface was a promising method of improving physio-chemical osseointegration of Ti-based prostheses to host bones, because such a coating could directly induce bone formation on its surface, improve bone-implant contact, reduce implant loosening and alleviate other adverse reactions such as the toxic effects of Ti ions released from the prosthesis [13, 15, 33].

Silicate or Si-doped ceramics were well documented that they could bond directly and tightly to surrounding bone because of their excellent bioactivity and the ability of inducing early bone formation *in vivo* [24, 37], and thus silicon-based ceramics have been widely used clinically as coatings so far. This phenomenon was ascribed to the formation of a bone-like apatite layer on their surface in virtue of a dissolution-precipitation-transformation mechanism, which is thought to be an essential condition for direct bonding formation [4, 8, 14, 30, 38]. By now, many researchers thought that bioactivity not only lay in the chemical bonding of implant to the surrounding bone tissue, but also rested with the ability of stimulating some special cellular reactions and promoting bone osteogenesis at molecular level. The ionic products released from silicate ceramics could provide an ideal physiological micro-environment for cellular reaction and colonization of bone-related cells, and influence cell cycle as well as its function expression, which gave rise to a tissue response termed osteoconduction and osteoinduction in which bone directly grew on and bonded to the coating, and finally promoted new bone regeneration [39, 40, 41].

In clinical practice, akermanite, a CaO–MgO–SiO_2-based bioceramic, has been demonstrated to be able to promote bone remodelling and angiogenesis *in vivo,* which further proved the above inference [10]. Because of the similarity in chemical composition, M2 might also possessed analogous biological properties. Moreover, its CTE was closer to Ti–6Al–4V alloy [22, 23], so M2 might be used as a prospective coating on Ti–6Al–4V substrate. Base on the above mentioned, histological analysis was used to verify whether the bioactivity and biocompatibility of M2 coated Ti–6Al–4V alloy were good enough to induce osteogenesis and promote the formation of direct bone-implant interface in osseointegration or not.

3.2. Histological study

With respect to performance *in vivo* of dense implants, three regions of interest can be distinguished through histological observation [42]: (i) interface, the morphology of host tissue directly adjacent to the implant is a measure for its bioactivity and biocompatibility; (ii) the surrounding tissue, tissue reaction is a response to both implantation procedure and presence of the implant, and (iii) implant, its histological appearance can reveal information with regards to the stability and integrity.

There are two common types of bonding at the bone-implant interface: indirect bonding and direct bonding [43]. A good example for the former type lies in titanium implant. Bio-inert titanium prosthesis was not directly adjacent to host bone tissue, but was encapsulated by fibrous tissues that isolated them from the surrounding bone. On the other hand, direct bone-implant interface was also known as chemical bone-bonding interface, which arised from the direct growth of bone tissue on the bioactive surface. This interface was expected to be free of any evidence of chronic inflammatory response and fibrous connective tissue formation. Moreover, osteoblasts, osteoid and minerals could be observed near this kind of interface [14]. The formation of a direct interface was crucial to osseointegration and long-term stability *in vivo* of implants [34, 36, 37].

Osseointegration is defined as the formation of a direct structural and functional connection between the implant and the bone tissues without fibrous tissue interposition at the optical microscopy level [43], Which is also the result of the osteoconduction of the implant system. Now it has emerged as the criterion used to evaluate the initial viability, stability as well as long-term success of implants. In addition, the bioactivity is extremely crucial for osteoinductivity and osteogenesis [38]. Since successful osseointegration of the implant surface is closely related to the quality and quantity of the new bone formed around implant, the outstanding bioactivity of implant is also particularly important for eventual successful osseointegration [31, 44, 45].

Based on the above background knowledge, histological observation was employed to evaluate the osteogenic ability and osseointegration of M2 coated Ti–6Al–4V implant. Fig. 5 displays the histological morphologies of bone-implant sections of M2-coated Ti–6Al–4V alloy and the control with toluidine-blue staining and double fluorescent labeling after implantation in rabbit femoral defect model for 1, 2 and 3 months. In general, new bone formed and bonded to both types of implants directly, and inflammation and other foreign body reaction such as formation of intervene fibrous tissue were not observed. However, bony tissue surrounding the M2 coated Ti6Al4V alloy implant was better-established than the control.

Results from a comparative analysis of 1-month optical micrographs of the experimental and control groups show that, a mass of new bone with embedded osteocytes was formed directly along the surface of M2 coated Ti–6Al–4V alloy implant, and no gap at light microscopic level was observed between the implant and bone tissue after implantation for 1 month. Blood vessels or medullary cavity had emerged in the newly formed bone. Besides, the boundary between the old and newly formed bone was quite clear. Compared with the old bone, osteocytes in osseous lacuna were smaller and irregularly distributed in osteoid matrix of the newly formed bone as illustrated in Fig. 5a1. This phenomenon indicated that the outside surface of M2 coated Ti–6Al–4V implant presented active region, where the osteogenesis process originated, and the chemistry and morphology of the interface at 1 month had been already remodeling well in progress. On the contrary, the amount of newly formed bone around HA coated Ti–6Al–4V implant was significantly smaller than the experimental implant. The control implant was separated from the host bone in the procedure of preparing slices, showing a poor osseointegration capacity to the host bone. Moreover, a large proportion of HA coating was broken away from the titanium alloy substrate, and only a small part of the HA coating was bonded to the host bone tissue, displaying a lower bond strength with titanium alloy substrate (Fig. 5b1). The above results were accordant with our previous study about bonding strength between the ceramic coating and titanium alloy substrate [23].

Chronic low-grade inflammation was not observed in both groups after two months of implantation. New bone layer contacted intimately with the outside surface of M2 coated Ti6Al4V alloy became noticeably thicker and more continuous, and the characteristic mechanical interlocking pattern at the interface was formed. Angiogenesis in the early period of bone healing was observed, and the arrangement of osteocytes was much more regular. The mineralization degree and structure maturity of newly formed bone were gradually increased with time (Fig. 5a2). In the control group, as displayed in Fig. 5b2, although the newly formed bone surrounding HA coated Ti–6Al–4V alloy was also further developed, its maturity degree was lower, and their structures and morphologies were similar to the experimental group at the time-point of 1 month.

Ordinary optical micrographs (Fig. 5a3 and b3) of tissue sections at 3 month also clearly displayed that the mineralization degree of newly formed bony tissue surrounding the experimental implant was quite high, and the newborn bony tissue was rich in new blood vessels and mature bone lacuna at the late stage of the implantation. Haversian canal and woven bone composed of bone lacunae and osteocytes were clearly visible, and bone trabecular had been formed in the surrounding bone tissue. Besides, some long strips of immature bone tissue with low calcification degree were closely connected to the M2 coated Tl–6Al–4V alloy (Fig. 5a3). While in the case of the control implants of the same

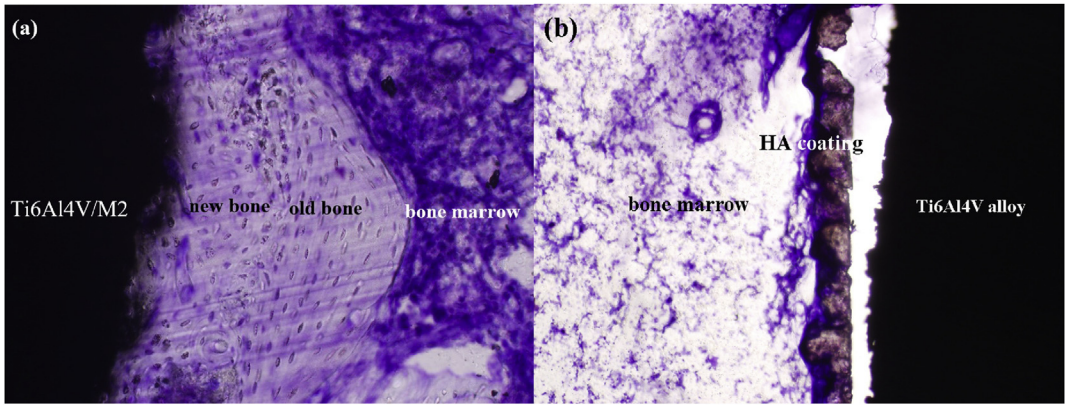

Fig. 6. The ability to induce osteogensis of M2 and HA coatings on Ti6Al4V alloy in bone marrow after 3 months in rabbit. (a) M2 coating; (b) HA coating.

period, as shown in Fig. 5b3, the mineralization degree of new bone around the implant was also high, yet its thickness and amount were obviously smaller, and there was no bone-like substance of low-maturity was found as the experimental group showed in Fig. 5a3. It is also noteworthy that, at 3 months time point, the contact ratio and area of mineralized bone between the implant and bone were significantly greater in the experimental group than that in the control group.

Administered *in vivo*, calcium-binding fluorescent dyes are anabolic time markers of osteogenesis and bone remodeling. During osteogenic and mineralisation process of the bone, the fluorescent dyes were combined with calcium and absorbed into the surface of hydroxyapatite crystals or within the crystal lattice, which could mark the formation process of new bone. Histomorphometric analysis of label incidence is an effective method of assessing the osteogenic activity and mineralization degree of newly formed active bony tissue around the implants, and reflecting the state of bone remodeling [39, 44, 46]. Tetracycline and calein could combine with newly calcified bone or amorphous calcium phosphate in the primary phase of bone mineralization. Moreover, the deposition of tetracycline and calcein drugs in bone depended on their absorption by new bony tissue. Therefore, this method could be used to evaluate the osteogenetic activity and quantity of new bone formed around the implants in this study.

Fig. 5a3-P and b3-P display the fluorescence microscopy images of the corresponding implant-bone sections under the same view field of both groups at month 3. Almost no obvious fluorescent signal was observed around HA coated Ti6Al4V alloy implants (Fig.5b3-P), while the experimental group showed a significantly stronger fluorescent signal marking the active bony tissue surrounding the M2 coated Ti6Al4V alloy implant (Fig.5a3-P). The Fluorescent substance was distributed in the M2 coating or throughout the newly formed bone around the implant with a spotted or flaky or clustered character.

Fig. 6 displays the ability of inducing osteogenesis of both types of implants in bone marrow after implantation in marrow cavity for 3 months. It could be obviously seen from Fig. 6a, the new bone had been formed and closely combined with M2 coating without optically visible gap, while there was no obvious newly formed bone around HA coating (Fig. 6b). In another word, the experimental group showed faster and more effective osteogenesis at the defect area than the control.

The above results indicated that, after implantation for 3 month, new bone was being actively and directly formed on or into M2 coatings, and its quantity were larger than HA coating, showing faster and more effective osteogenesis and osteointegration in the defect area. In another word, M2 coating possessed higher osteoinductive and osteoconductive ability, and it might be much more appropriate for osseointegration and bone remodelling than HA coating. This phenomenon also supported an adequate bioactivity and biocompatibility *in vivo* of M2 coated Ti–6Al–4V alloy.

In essence, the above favourable histological performance of M2 coated Ti–6Al–4V alloy may be attributed to the following reasons. As our previous studies [22, 23] have shown, Mg, and silicon ions were gradually released from M2 coating on Ti–6Al–4V substrate, but not in the control group. Mg and Si ions could activate the expression of bone related genes, enhance osteoblast adhesion and proliferation to stimulate bone formation, mineralization and angiogenesis [4, 10, 13, 47], thus they might play a positive role in promoting the formation of new bony tissue around the M2 coated Ti–6Al–4V alloy, while HA coating did not exhibited this performance.

4. Conclusion

In this research, New Zealand rabbit femoral defect model was employed to evaluated the performance *in vivo* of CaO–MgO–SiO_2–based bioactive glass-ceramic M2 coated Ti–6Al–4V implant, with commercial HA coating/Ti6Al4V as the control. After surgery, the wound healed well in operation area. Toxic and foreign body reaction, material exposure and tissue necrosis were not observed. M2 coated Ti6Al4V alloy was biocompatible with its surrounding muscle tissue. A large amount of new bone generated around the implants, and an intimate bone integration was formed at the interface, indicating outstanding osteointegration characteristic. This novel implant could also induce new bone formation in the bone marrow, and its ability to induce osteogenesis was much higher than the control. In summary, from all the results, it was verified that the M2 coatedTi6Al4V possessed better biological performance *in vivo*, and might take the place of HA coated Ti6Al4V in repairing load-bearing bone defects in the future.

Declarations

Author contribution statement

Mengjiao Zhang, Xianchun Chen: Conceived and designed the experiments; Performed the experiments; Contributed reagents, materials, analysis tools or data; Wrote the paper.

Ximing Pu: Analyzed and interpreted the data.

Guangfu Yin: Contributed reagents, materials, analysis tools or data.

Funding statement

This work was supported by the National Natural Science Foundation of China (project Nos. 51872190) and the Fundamental of Research Funds for the Central University (SCU2017A001 & 2018SCUH0024).

Competing interest statement

The authors declare no conflict of interest.

Additional information

No additional information is available for this paper.

References

[1] S.V. Gnedenkov, S.L. Sinebryukhov, A.V. Puz, V.S. Egorkin, R.E. Kostiv, In vivo study of osteogenerating properties of calcium-phosphate coating on titanium alloy Ti-6Al-4V, Biomed. Mater. Eng. 27 (6) (2016) 551–560.

[2] K.Y. Hung, S.C. Lo, C.S. Shih, Y.C. Yang, H.P. Feng, Y.C. Lin, Titanium surface modified by hydroxyapatite coating for dental implants, Surf. Coat. Technol. 231 (2013) 337–345.

[3] X.L. Zeng, J.F. Li, S.H. Yang, Q.X. Zheng, Z.W. Zou, Preparation of artificial canine femoral stem with HA-Ti ladder-type coating on plasma-sprayed pure Ti substrate and its performance evaluation, Appl. Surf. Sci. 258 (2012) 4489–4496.

[4] J.L. Xu, D. Joguet, J. Cizek, K.A. Khor, H.L. Liao, C. Coddet, W.N. Chen, Synthesis and characterization on atomphospheric plasma sprayed amorphous silica doped hydrxoyapatite coatings, Surf. Coat. Technol. 206 (2012) 4659–4665.

[5] Y.C. Yang, Influence of residual stress on bonding strength of the plasma-sprayed hydroxyapatite coating after the vacuum heat treatment, Surf. Coat. Technol. 201 (2007) 7187–7193.

[6] R.A. Surmenev, A review of plasma-assisted methods for calcium phosphate-based coatings fabrication, Surf. Coat. Technol. 206 (8–9) (2012) 2035–2056.

[7] J.H. Lee, Hae L. Jang, K.M. Lee, H.R. Baek, K. Jin, Kug S. Hong, J.H. Noh, H.K. Lee, *in vitro* and in vivo evaluation of the bioactivity of hydroxyapatite coated polyetheretherketone biocomposites created by cold spray technology, Acta Biomater. 9 (2013) 6177–6187.

[8] J.Y. Sun, L. Wei, X.Y. Liu, J.Y. Li, B.E. Li, G.C. Wang, F.H. Meng, Influences of ionic dissolution products of dicalcium silicate coating on osteoblastic proliferation, differentiation and gene expression, Acta Biomater. 5 (2009) 1284–1293.

[9] M.N. Rahaman, D.E. Day, B.S. Bal, Q. Fu, S.B. Junga, L.F. Bonewald, A.P. Tomsia, Bioactive glass in tissue engineering, Acta Biomater. 7 (6) (2011) 2355–2373.

[10] Y. Huang, X.G. Jin, Xi.L. Zhang, H.L. Sun, J.W. Tu, T.T. Tang, J. Chang, K.R. Dai, In vitro and in vivo evaluation of akermanite bioceramics for bone regeneration, Biomaterials 30 (2009) 5041–5048.

[11] S. Naseri, S.N. Nazhat, 14: bioactive and soluble glasses for wound-healing applications, Bioactive Glasses, second ed., 2018, pp. 381–405.

[12] Z. Muhammad, F. Imran, A. Muhammad, N. Shariq, K. Ohaib, Z. Sana, Chapter 11: Bioactive Surface Coatings for Enhancing Osseointegration of Dental Implants, Biomedical, Therapeutic and Clinical Applications of Bioactive Glasses, 2019, pp. 13–329.

[13] J.R. Henstock, L.T. Canham, S.I. Anderson, Silicon: the evolution of its use in biomaterials, Acta Biomater. 11 (2015) 17–26.

[14] J.Y. Sun, J.Y. Li, X.Y. Liu, L. Wei, G.C. Wang, F.H. Meng, Proliferation and gene expression of osteoblasts cultured in DMEM containing the ionic products of dicalcium silicate coating, Biomed. Pharmacother. 63 (2009) 650–657.

[15] H.J. Gu, F.F. Guo, X. Zhou, L.L. Gong, Y. Zhang, W.Y. Zhai, L. Chen, L. Cen, S. Yin, J. Chang, L. Cui, The stimulation of osteogenic differentiation of human adipose-derived stem cells by ionic products from akermanite dissolution via activation of the ERK pathway, Biomaterials 32 (2011) 7023–7033.

[16] A. Hoppe, N. Güldal, A.R. Boccaccini, A review of the biological response to ionic dissolution products from bioactive glasses and glass-ceramics, Biomaterials 32 (11) (2011) 2757–2774.

[17] W.Y. Zhai, H.X. Lu, C.T. Wu, L. Chen, X.L. Lin, K. Naoki, G.P. Chen, J. Chang, Stimulatory effects of the ionic products from Ca-Mg-Si bioceramics on both osteogenesis and angiogenesis in vitro, Acta Biomater. 9 (2013) 8004–8014.

[18] S.T. Neda, F.V. Megen, J.B. Timothy, K.L. Kelly, S.B. Nicole, W.M. Grayson, M.L. Peter, B.A. Pranesh, G.V. Venu, Combinatorial effect of $Si4+$, $Ca2+$, and $Mg2+$ released from bioactive glasses on osteoblast osteocalcin expression and biomineralization, Mater. Sci. Eng. C 33 (5) (2013) 2757–2765.

[19] M. Shamsi, M. Karimi, M. Ghollasi, N. Nezafati, M. Shahrousvand, M. Kamali, A. Salimi, In vitro proliferation and differentiation of human bone marrow mesenchymal stem cells into osteoblasts on nanocomposite scaffolds based on bioactive glass ($64SiO_2$-$31CaO$-$5P_2O_5$)-poly-l-lactic acid nanofibers fabricated by electrospinning method, Mater. Sci. Eng. C 78 (2017) 114–123.

[20] Y.L. Zhou, C.T. Wu, J. Chang, Bioceramics to regulate stem cells and their microenvironment for tissue regeneration, Mater. Today 24 (2019) 41–56.

[21] E. O'Neill, G. Awale, L. Daneshmandi, O. Umerah, K.W.H. Lo, The roles of ions on bone regeneration, Drug Discov. Today 23 (4) (2018) 879–890.

[22] X.C. Chen, X.M. Liao, Z.B. Huang, P.L. You, C. Chen, Y.Q. Kang, G.F. Yin, Synthesis and characterization of novel multiphase bioactive glass-ceramics in the CaO-MgO-SiO2 system, J. Biomed. Mater. Res. B Appl. Biomater. 93B (2010) 194–202.

[23] X.C. Chen, M.J. Zhang, X.M. Pu, G.F. Yin, X.M. Liao, Z.B. Huang, Y.D. Yao, Characteristics of heat-treated plasma-sprayed CaO–MgO–SiO_2-based bioactive glass–ceramic coatings on Ti–6Al–4V alloy, Surf. Coat. Technol. 249 (2014) 97–103.

[24] P.N. De Aza, Z.B. Luklinska, C. Santos, F. Guitian, S. De Aza, Mechanism of bone-like formation on a bioactive implant in vivo, Biomaterials 24 (8) (2003) 1437–1445.

[25] W. Zheng, GB/T 16886.1–2011: Translated English PDF of Chinese Standard GB/T16886. 1-2011: Biological Evaluation of Medical Devices-Part 1: Evaluation and Testing within a Risk-Management Process (GBT16886. 1-2011; GBT 16886.1-2011) [M], 2014. www.ChineseStandard.net.

[26] J.X. Lu, A. Gallur, B. Flautre, K. Anselme, M. Descamps, B. Thierry, Comparative study of tissue reactions to calcium phosphate ceramics among cancellous, cortical, and medullar bone sites in rabbits, J. Biomed. Mater. Res. 42 (3) (1998) 357–367.

[27] A.P. Marques, R.E. Reis, J.A. Hunt, The biocompatibility of novel starch based polymers and composites: in vitro studies, Biomaterials 23 (6) (2002) 1471–1478.

[28] J.K. Actor, Chapter 2: the Inflammatory Response. Introductory Immunology, second ed., 2019, pp. 17–30.

[29] A. Dalu, L.G. Lomax, K.B. Delclos, B.S. Blaydes, A comparison of the inflammatory response to a polydimethylsiloxane implant in male and female Balb/c mice, Biomaterials 21 (19) (2000) 1947–1957.

[30] F.R. Pu, R.L. Williams, T.K. Markkula, J.A. Hunt, Expression of leukocyte-endothelial cell adhesion molecules on monocyte adhesion to human endothelial cells on plasma treated PET and PTFE in vitro, Biomaterials 23 (24) (2002) 4705–4718.

[31] J. Gil-Albarova, R. Garrido-Lahiguera, A.J. Salinas, J. Román, A.L. Bueno-Lozano, R. Gil-Albarova, M. Vallet-Regí, The in vivo performance of a sol–gel glass and a glass-ceramic in the treatment of limited bone defects, Biomaterials 25 (2004) 4639–4645.

[32] S. Yu, Z.T. Yu, G. Wang, J.Y. Han, X.Q. Ma, M.S. Dargusch, Biocompatibility and osteoconduction of active porous calcium-phosphate films on a novel Ti–3Zr–2Sn–3Mo–25Nb biomedical alloy, Colloids Surfaces B Biointerfaces 85 (2011) 103–115.

[33] V.M. da Rocha Barros, L.A. Salata, C.E. Sverzut, S.P. Xavier, R. van Noort, A. Johnson, P.V. Hatton, In vivo bone tissue response to a canasite glass-ceramic, Biomaterials 23 (2002) 2895–2900.

[34] Y.Z. Huang, S.K. Hea, Z.J. Guo, J.K. Pi, L. Deng, L. Dong, Y. Zhang, B. Su, L.C. Da, L. Zhang, Z. Xiang, W. Ding, M. Gong, H.Q. Xie, Nanostructured titanium surfaces fabricated by hydrothermal method: influence of alkali conditions on the osteogenic performance of implants, Mater. Sci. Eng. C 94 (2019) 1–10.

[35] Z.J. Guo, N. Jiang, C. Chen, S.S. Zhu, L. Zhang, Y.B. Li, Surface bioactivation through the nanostructured layer on titanium modified by facile HPT treatment, Sci. Rep. 7 (2017) 1–11.

[36] C. Pierre, G. Bertrand, C. Rey, O. Benhamou, C. Combes, Calcium phosphate coatings elaborated by the soaking process on titanium dental implants:Surface preparation, processing and physical–chemical characterization, Dent. Mater. 35 (2) (2019) 25–35.

[37] F. Romero-Gavilan, N. Araújo-Gomes, A.M. Sánchez-Pérez, I. García-Arnáez, F. Elortza, M. Azkargorta, J.J. Martín de Llano, C. Carda, M. Gurruchaga, J. Suay, I. Goni, Bioactive potential of silica coatings and its effect on the adhesion of proteins to titanium implants, Colloids Surfaces B Biointerfaces 162 (2018) 316–325.

[38] M. Łączka, K. Cholewa-Kowalska, A.M. Osyczka, Bioactivity and osteoinductivity of glasses and glassceramics and their material determinants, Ceram. Int. 42 (13) (2016) 14313–14325.

[39] C. Domínguez-Trujillo, F. Ternero, J.A. Rodríguez-Ortiz, S. Heise, A.R. Boccaccini, J. Lebrato, Y. Torres, Hierarchical micropore/nanorod apatite hybrids in-situ grown from 3-D printed macroporous Ti6Al4V implants with improved bioactivity and osseointegration, J. Mater. Sci. Technol. 33 (2) (2017) 179–186.

[40] C.T. Wu, Z.T. Chen, Q.J. Wu, D.L. Yi, T. Friis, X.B. Zhen, J. Chang, X.Q. Jiang, Y. Xiao, Clinoenstatite coatings have high bonding strength, bioactive ion release, and osteoimmunomodulatory effects that enhance in vivo osseointegration, Biomaterials 71 (2015) 35–47.

[41] X.M. Liu, M. Li, Y.Z. Zhu, K.W.K. Yeung, P.K. Chu, S.L. Wu, Roles of calcium ion in osteoinductions, the modulation of stem cell behaviors by functionalized nanoceramic coatings on Ti-based implants, Bioact. Mater. 1 (2016) 65–76.

[42] S.C. Mendes, R.L. Reis, Y.P. Bovell, A.M. Cunha, A.V.B. Clemens, J.D. de Bruijn, Biocompatibility testing of novel starch-based materials with potential application in orthopaedic surgery: a preliminary study, Biomaterials 22 (2001) 2057–2064.

[43] V. Goriainov, R. Cook, J.M. Latham, D.G. Dunlop, R.O.C. Oreffo, Bone and metal: an orthopaedic perspective on osseointegration of metals, Acta Biomater. 10 (2014) 4043–4057.

[44] H.Y. Liu, H. Zheng, X.P. Hou, W.J. Zhong, X.X. Ying, S.L. Chai, G.W. Ma, Bio-Oss® for delayed osseointegration of implants in dogs: a histological study, Br. J. Oral Maxillofac. Surg. 52 (2014) 729–734.

[45] P.G. Coelho, R. Jimbo, Osseointegration of metallic devices: current trends based on implant hardware design, Arch. Biochem. Biophys. 561 (2014) 99–108.

[46] C. Pautke, S. Vogt, T. Tischer, G. Wexel, H. Deppe, S. Milz, M. Schieker, A. Kolk, Poly chrome labeling of bone with seven different fluorochromes: enhancing fluorochrome discrimination by spectral image analysis, Bone 37 (2005) 441–445.

[47] H. Zreiqat, C.R. Howlett, A. Zannettino, P. Evans, G. Schulze-Tanzil, C. Knabe, M. Shakibae, Mechanisms of magnesium-stimulated adhesion of osteoblastic cells to commonly used orthopaedic implants, J. Biomed. Mater. Res. 62 (2002) 175–184.